Acta Crystallographica Section A
Foundations of Crystallography
ISSN 0108-7673

Received 30 November 2002
Accepted 13 January 2003

© 2003 International Union of Crystallography
Printed in Great Britain – all rights reserved

A universal computation method for two-beam dynamical X-ray diffraction

XianRong Huang* and Michael Dudley

Department of Materials Science and Engineering, State University of New York at Stony Brook, Stony Brook, NY 11794-2275, USA. Correspondence e-mail: xiahuang@ms.cc.sunysb.edu

A general-purpose method that includes nearly all possible two-beam diffraction mechanisms is presented for calculating diffracted and specularly reflected X-ray intensities from single crystals. Based on this method, it is demonstrated that a small universal computational routine can be developed to accurately treat two-beam diffraction for any scattering geometry.

Compared with the kinematical theory, dynamical X-ray diffraction theory is a more accurate model for single-crystal diffraction (Authier, 2001). For the two-beam case, the fundamental equations of dynamical theory are Laue's wave equations

$$\begin{aligned}\frac{k_0^2 - K^2}{k_0^2} D_0 &= \chi_0 D_0 + C\chi_{\bar{h}} D_h,\\ \frac{k_h^2 - K^2}{k_h^2} D_h &= \chi_0 D_h + C\chi_h D_0,\end{aligned} \tag{1}$$

where $K = |\mathbf{K}_0| = \omega/c$ is the wavenumber of the incident wave in vacuum ($\mathbf{K}_0$ the wavevector), k_0 and k_h are the scalar values of the refracted and diffracted wavevectors $\mathbf{k}_0$ and $\mathbf{k}_h$ inside the crystal, respectively, C is the polarization factor, and the other symbols have well known meanings (Pinsker, 1978). The internal wavevectors are related to the incident wavevector $\mathbf{K}_0$ by

$$\begin{aligned}\mathbf{k}_0 &= \mathbf{K}_0 + K\delta\mathbf{n},\\ \mathbf{k}_h &= \mathbf{k}_0 + \mathbf{h} = \mathbf{K}_0 + \mathbf{h} + K\delta\mathbf{n},\end{aligned} \tag{2}$$

where $\mathbf{h}$ is the diffraction vector ($|\mathbf{h}| = 2\pi/d$, d the spacing of the diffracting planes), $\mathbf{n}$ is the inward unit normal to the crystal surface and δ is a small complex quantity (Laue, 1960). The first equation in (2) is based on the requirement that the tangential components of $\mathbf{k}_0$ and $\mathbf{K}_0$ with respect to the surface be identical.

Based on the linearization approximation

$$[k_m^2(1 - \chi_0) - K^2]/k_m^2 \simeq [2k_m - K(2 + \chi_0)]/K$$

(for $m = 0, h$), the secular equation (*i.e.* dispersion equation) of (1) becomes a quadratic equation, from which a two-wavefield model was first established in literature, which constitutes the classical dynamical theory. Afterwards, a variety of extensions to this model (which form the so-called 'extended dynamical theory') has been developed to treat special cases where one or other of the approximations used in the two-wavefield model fails (*e.g.* Bedynska, 1973; Härtwig, 1978; Afanas'ev & Melkonyan, 1983; Caticha, 1993; De Caro *et al.*, 1997; De Caro & Tapfer, 1997; Authier, 1998). However, most of these four-wavefield models still lack generality. Apart from a number of unnecessary (or unreasonable) approximations, a frequent mistake made in the extended theory is that the polarization factor C of π polarization is regarded as a constant ($= \cos 2\theta_B$, θ_B the Bragg angle). In fact, this assumption is valid only when the diffraction angle is close to θ_B (while the corresponding models are usually supposed to be valid in wide angular ranges).[1] The other common limitation of the previous extensions is that they are generally modeled only for coplanar diffraction geometry (or for non-coplanar geometry, but not for both).

In the following, we will elaborate a straightforward and universal method to strictly solve equations (1) based on (2) and some useful results of the previous extensions.

The exact dispersion equation indicated by (1) is apparently

$$(k_0^2\chi_p - K^2)(k_h^2\chi_p - K^2) = C^2 k_0^2 k_h^2 \chi_h \chi_{\bar{h}}, \tag{3}$$

where $\chi_p = 1 - \chi_0$. From (2), k_0^2 ($= \mathbf{k}_0 \cdot \mathbf{k}_0$) and k_h^2 ($= \mathbf{k}_h \cdot \mathbf{k}_h$) can be derived as

$$\begin{aligned}k_0^2 &= K^2(1 + 2\gamma_0\delta + \delta^2),\\ k_h^2 &= K^2[\alpha + 2(\gamma_0 + \varphi_h)\delta + \delta^2],\end{aligned} \tag{4}$$

where $\varphi_h = \mathbf{n} \cdot \mathbf{h}/K$ is a constant and γ_0 is the cosine of the angle between $\mathbf{K}_0$ and $\mathbf{n}$. For an arbitrary incidence direction $\mathbf{s}_0$ ($= \mathbf{K}_0/K$), we have

$$\gamma_0 = \gamma_0(\mathbf{s}_0) = \mathbf{s}_0 \cdot \mathbf{n}. \tag{5}$$

The parameter α in (4) is also a function of $\mathbf{s}_0$:

$$\alpha = \alpha(\mathbf{s}_0) = |\mathbf{s}_0 + \mathbf{h}/K|^2. \tag{6}$$

Note that, for π polarization, the polarization factor C is exactly equal to the cosine of the angle between $\mathbf{k}_0$ and $\mathbf{k}_h$ (inside the crystal), *i.e.* $C_\pi = (\mathbf{k}_0 \cdot \mathbf{k}_h)/(k_0 k_h)$. So, in a rigorous way, we have $C_\sigma \equiv 1$ for σ polarization and

$$k_0 k_h C_\pi = \mathbf{k}_0 \cdot \mathbf{k}_h = K^2[\beta + (2\gamma_0 + \varphi_h)\delta + \delta^2] \tag{7}$$

[1] Mathematically, $C = \cos 2\theta_B$ is incorrect even when the diffraction angle is close to θ_B since the polarization factors of the four wavefields may be quite different (see Fig. 3 in the following).

for π polarization. Here (7) is again based on (2), and β is related to $\mathbf{s}_0$ by

$$\beta = \beta(\mathbf{s}_0) = 1 + \mathbf{s}_0 \cdot \mathbf{h}/K. \tag{8}$$

For σ polarization, inserting (4) into (3), one can write the exact dispersion equation in a quartic form:

$$\delta^4 + A_1\delta^3 + A_2\delta^2 + A_3\delta + A_4 = 0, \tag{9}$$

with the four coefficients being

$$\begin{aligned} A_1 &= 4\gamma_0 + 2\varphi_h, \\ A_2 &= 4\gamma_0(\gamma_0 + \varphi_h) + \alpha + 1 - 2\chi_p/A_0, \\ A_3 &= 2\gamma_0(\alpha + 1) + 2\varphi_h - \chi_p A_1/A_0, \\ A_4 &= \alpha - (\alpha\chi_p - \chi_0)/A_0, \end{aligned} \tag{10}$$

where $A_0 = \chi_p^2 - \chi_h\chi_{\bar{h}}$. For π polarization, we insert both (4) and (7) into (3). The resultant dispersion equation still has the quartic form (9), but the coefficients become

$$\begin{aligned} A_1^\pi &= 4\gamma_0 + 2\varphi_h, \\ A_0A_2^\pi &= \chi_p^2[4\gamma_0(\gamma_0 + \varphi_h) + \alpha + 1] \\ &\quad - 2\chi_p - \chi_h\chi_{\bar{h}}[(A_1^\pi/2)^2 + 2\beta], \\ A_0A_3^\pi &= 2\chi_p^2[\gamma_0(\alpha + 1) + \varphi_h] - (\chi_p + A_1^\pi\chi_h\chi_{\bar{h}}\beta), \\ A_0A_4^\pi &= \chi_0(1 - \alpha\chi_p) - \chi_h\chi_{\bar{h}}\beta^2. \end{aligned} \tag{11}$$

In classical dynamical theory, γ_0 is assumed to be constant while the effective incidence direction is expressed by $\Delta\theta$, the deviation of the incidence angle θ from the Bragg angle θ_B. In this paper, however, γ_0 and the other two parameters, α and β, are strictly treated as functions of $\mathbf{s}_0$ so that $\Delta\theta$ is not needed. Moreover, most of the conventional constants, such as θ_B, $\sin 2\theta_B$, $\cos 2\theta_B$, and the asymmetry factor b are not used here. As a result, the related approximations are completely removed. The use of vector $\mathbf{s}_0$ instead of the scalar parameter $\Delta\theta$ as the input also indicates that the diffraction process is modeled in three-dimensional space (while the classical treatment is generally limited within the incidence plane).

The complex-coefficient equation (9) may be analytically solved (see *e.g.* Weisstein, 1999) with the aid of

$$x^3 + 3px + 2q = 0, \tag{12}$$

where

$$\begin{aligned} p &= \frac{A_1A_3}{12} - \frac{A_2^2}{36} - \frac{A_4}{3}, \\ q &= \frac{A_2(A_1A_3 - 4A_4)}{48} - \frac{A_2^3}{216} + \frac{A_4(4A_2 - A_1^2) - A_3^2}{16}. \end{aligned} \tag{13}$$

The roots of (12) have the form

$$x = w - p/w, \tag{14}$$

where

$$w = \exp(i2n\pi/3)[-q \pm (q^2 + p^3)^{1/2}]^{1/3} \tag{15}$$

for $n = 0, 1, 2$. Although w may have six different values, these values lead to at most three different values of x through (14). Thus, only one of the '$\pm$' signs in (15) is necessary, but the one that corresponds to a larger $|w|$ must be selected. Then, one may use the parameters

$$\begin{aligned} y &= x + A_2/6, & z_1 &= (8y + A_1^2 - 4A_2)^{1/2}, \\ z_2 &= (A_1 + z_1)/2, & z_3 &= y + (A_1y - A_3)/z_1, \\ z_4 &= (A_1 - z_1)/2, & z_5 &= y - (A_1y - A_3)/z_1 \end{aligned} \tag{16}$$

to express the four roots of (9) as:

$$\begin{aligned} \delta_{1,2} &= \frac{-z_2 \pm (z_2^2 - 4z_3)^{1/2}}{2}, \\ \delta_{3,4} &= \frac{-z_4 \pm (z_4^2 - 4z_5)^{1/2}}{2}. \end{aligned} \tag{17}$$

In (16), x can be, in principle, any root of (12). In order to minimize possible computational errors, however, the root that makes $|z_1|$ maximum must be chosen. Meanwhile, one may use

$$[r\exp(i\phi)]^{1/n} = r^{1/n}\exp(i\phi/n)$$

to calculate the square or cube roots in (15)–(17), where $r\exp(i\phi)$ is the phasor form of a complex number ($r > 0$ and $0 \le \phi < 2\pi$). After the dispersion equation (3) is strictly solved, we may obtain from (2) the internal wavevectors $\mathbf{k}_0^{(j)}$ and $\mathbf{k}_h^{(j)}$ ($j = 1, 2, 3, 4$). Meanwhile, $(k_m^{(j)})^2$ can be calculated from (4), and $k_m^{(j)}$ is the square root of $(k_m^{(j)})^2$ with a positive real part ($m = 0, h$ and $j = 1, 2$).[2] Afterwards, the polarization factor for π polarization can be calculated from its definition, $C_\pi^{(j)} = (\mathbf{k}_0^{(j)} \cdot \mathbf{k}_h^{(j)})/(k_0^{(j)}k_h^{(j)})$. Note that these treatments make $k_m^{(j)}$ and $C_\pi^{(j)}$ all complex, but the imaginary parts of these quantities are so small that they have no noticeable effects in the following treatment of boundary conditions.

Naturally, four wavefields ($D_0^{(j)}$, $D_h^{(j)}$) may exist in the crystal and the amplitude ratio $r_j = D_h^{(j)}/D_0^{(j)}$ for each wavefield can be calculated from the second equation in (1) based on the corresponding δ_j (since the first equation may give computational errors when $\theta_B \sim 45^\circ$ for π polarization). The strengths of these wavefields are determined by the boundary conditions at the surface: the continuity of the tangential components (parallel to the surface) of the electric fields $\mathbf{E}$ and the magnetic fields $\mathbf{H}$ (Holý, 1996). To use the $\mathbf{E}$-wave boundary conditions, one has to convert the $\mathbf{D}$ fields inside the crystal into $\mathbf{E}$ fields. Based on $\mathbf{E} \simeq (1 - \chi)\mathbf{D}$ (c.g.s. units), their relations for the two-beam case are

$$\mathbf{E}_0^{(j)} \simeq \chi_p\mathbf{D}_0^{(j)} - \chi_{\bar{h}}\mathbf{D}_h^{(j)}, \quad \mathbf{E}_h^{(j)} \simeq \chi_p\mathbf{D}_h^{(j)} - \chi_h\mathbf{D}_0^{(j)}. \tag{18}$$

Meanwhile, the magnetic field $\mathbf{H}$ can be derived from one of Maxwell's equations, $\nabla \times \mathbf{H} = (1/c)(\partial\mathbf{D}/\partial t)$. This indicates that

$$\mathbf{H} = [\omega/(ck^2)]\mathbf{k} \times \mathbf{D} \tag{19}$$

for an arbitrary plane wave $\mathbf{D} = \mathbf{D}_0\exp(-i\mathbf{k} \cdot \mathbf{r} + i\omega t)$ (note that $\mathbf{D} \equiv \mathbf{E}$ in vacuum). Based on (18) and (19), one can

[2] Owing to absorption, any internal wavevector is a *complex vector* having the form $\mathbf{k} = k_r\mathbf{e}_k + ik_i\mathbf{n}$ with k_r and k_i being real and $\mathbf{e}_k$ a unit vector. For $\mathbf{e}_k \neq \mathbf{n}$, it follows that $\nabla \cdot \mathbf{D} \neq 0$ unless $\mathbf{D} \perp \mathbf{e}_k$ and $\mathbf{D} \perp \mathbf{n}$ (σ polarization). However, since $k_i/k_r \sim 10^{-6}$, one has $\nabla \cdot \mathbf{D} \simeq 0$ for π polarization with $\mathbf{D} \perp \mathbf{e}_k$. Strictly, $\mathbf{k}$ has no scalar value, but, as $k_i \ll k_r$, either k_r or the square root of $\mathbf{k} \cdot \mathbf{k}$ can be considered as the scalar value.

actually write the strict boundary conditions for any diffraction geometry.

To treat the boundary conditions in detail, let us consider the Bragg case for a semi-infinite crystal as an example. Then only two roots of (9) have negative imaginary parts, here denoted by δ_1 and δ_2 [but they do not necessarily correspond to the two roots in the first equation of (17)]. The other roots with positive imaginary parts must be discarded as they correspond to increasing amplitudes toward the inside of the crystal. Subsequently, there are two wavefields inside the crystal,

$$\mathbf{D}^{(j)} = \mathbf{D}_0^{(j)} \exp(-i\mathbf{k}_0^{(j)} \cdot \mathbf{r}) + \mathbf{D}_h^{(j)} \exp(-i\mathbf{k}_h^{(j)} \cdot \mathbf{r}),$$

with the corresponding electric fields being

$$\mathbf{E}^{(j)} = \mathbf{E}_0^{(j)} \exp(-i\mathbf{k}_0^{(j)} \cdot \mathbf{r}) + \mathbf{E}_h^{(j)} \exp(-i\mathbf{k}_h^{(j)} \cdot \mathbf{r}), \quad \text{for } j = 1, 2.$$

Above the crystal surface, there are three waves: the incident wave $\mathbf{E}_I \exp(-i\mathbf{K}_0 \cdot \mathbf{r})$, the specularly reflected wave $\mathbf{E}_R \exp(-i\mathbf{K}_R \cdot \mathbf{r})$ and the diffracted wave $\mathbf{E}_D \exp(-i\mathbf{K}_h \cdot \mathbf{r})$, with $|\mathbf{K}_0| = |\mathbf{K}_R| = |\mathbf{K}_h| = K$. Since the tangential components of $\mathbf{K}_0$, $\mathbf{k}_0^{(j)}$ and $\mathbf{K}_R$ are all the same, we have $K_{0z} = -K_{Rz} = K\gamma_0$ (axis z is along $\mathbf{n}$). Meanwhile, $\mathbf{K}_h$ can be calculated from

$$\begin{aligned} \mathbf{K}_{h\parallel} &= \mathbf{k}_{h\parallel} = \mathbf{k}_{0\parallel} + \mathbf{h}_\parallel = \mathbf{K}_{0\parallel} + \mathbf{h}_\parallel, \\ K_{hz} &= -(K^2 - |\mathbf{K}_{h\parallel}|^2)^{1/2}, \end{aligned} \tag{20}$$

where $\parallel$ indicates the tangential vector component with respect to the surface, $\mathbf{K}_{0\parallel} = K(\mathbf{s}_0 - \gamma_0\mathbf{n})$ and $\mathbf{h}_\parallel = K(\mathbf{h}/K - \varphi_h\mathbf{n})$.

For σ polarization, all the $\mathbf{E}$ and $\mathbf{D}$ vectors involved are parallel to each other. The four boundary conditions for the coplanar case ($\mathbf{K}_0$, $\mathbf{h}$ and $\mathbf{n}$ lying within the same plane) are (for a unit incidence $E_I = 1$)

$$\begin{aligned} 1 + E_R &= \sum_{j=1}^{2} (\chi_p - r_j\chi_{\bar{h}}) D_0^{(j)}, \\ E_D &= \sum_{j=1}^{2} (r_j\chi_p - \chi_h) D_0^{(j)}, \\ (K_{0z}/K^2)(1 - E_R) &= \sum_{j=1}^{2} [k_{0z}^{(j)}/(k_0^{(j)})^2] D_0^{(j)}, \\ (K_{hz}/K^2)E_D &= \sum_{j=1}^{2} [k_{hz}^{(j)}/(k_h^{(j)})^2] r_j D_0^{(j)}. \end{aligned} \tag{21}$$

The last two equations in (21) are based on the continuity of the tangential components of the magnetic fields $\mathbf{H}$. For π polarization in the coplanar case, the boundary conditions are

$$\begin{aligned} \gamma_0(1 - E_R) &= \sum_{j=1}^{2} (\chi_p\gamma_0^{(j)} - r_j\chi_{\bar{h}}\gamma_h^{(j)}) D_0^{(j)}, \\ \gamma_h E_D &= \sum_{j=1}^{2} (\chi_h\gamma_0^{(j)} - r_j\chi_p\gamma_h^{(j)}) D_0^{(j)}, \\ (1 + E_R)/K &= \sum_{j=1}^{2} (1/k_0^{(j)}) D_0^{(j)}, \\ E_D/K &= \sum_{j=1}^{2} (r_j/k_h^{(j)}) D_0^{(j)}, \end{aligned} \tag{22}$$

where $\gamma_h = K_{hz}/K$ and $\gamma_m^{(j)} = k_{mz}^{(j)}/k_m^{(j)}$ ($m = 0, h$). As both (21) and (22) are linear equation systems for the four unknowns $D_0^{(1)}$, $D_0^{(2)}$, E_D and E_R, they can be readily solved.

To test the above computational method, we consider 111 symmetric reflection from a semi-infinite silicon crystal (see the inset of Fig. 1) with σ polarization Cu $K\alpha_1$ radiation [$\lambda = 1.540562$ Å, $\chi_0 = -(15.16 + i0.3517) \times 10^{-6}$, $\chi_h = -(5.905 - i5.554) \times 10^{-6}$ and $\chi_{\bar{h}} = -(5.554 + i5.905) \times 10^{-6}$]. Within the incidence plane (containing $\mathbf{K}_0$ and $\mathbf{K}_h$), $\mathbf{s}_0 = \cos\theta\mathbf{x} + \sin\theta\mathbf{n}$, where θ is the incidence angle and $\mathbf{x}$ is a unit vector along axis x. Since $\mathbf{h}$ is normal to the crystal surface here ($\mathbf{h}_\parallel = 0$), $\mathbf{K}_h = \mathbf{K}_R$ according to (20). Thus, the scattering intensity detectable in experiments consists of contributions from both the diffracted and specularly reflected waves:

$$I_{D+R} = |E_D + E_R|^2. \tag{23}$$

Fig. 1 shows the calculated I_{D+R} as a function of θ. The intensity profile shows the typical characteristics of asymptotic Bragg diffraction [or truncation-rod scattering (Caticha, 1993)] over the entire angular range from 000 to 111 reflections. As plotted in the inset, the intensity profile in the small-angle range clearly reveals the phenomenon of total external reflection. Around the Bragg peak of 111 reflection, the asymmetric rocking curve correctly reveals the X-ray absorption effect. Note that in practice, when the incidence direction is far away from the Bragg angle, it may be necessary to consider the variation of the structure factors as a function of $\sin\theta/\lambda$. Meanwhile, it may also be necessary to analyze the contributions of other reflections in the framework of multiple-beam diffraction theory (Colella, 1991; Chien *et al.*, 1999). But these topics are beyond the scope of this paper.

A typical failure of the conventional dynamical theory is that it cannot properly treat the case where the Bragg angle θ_B

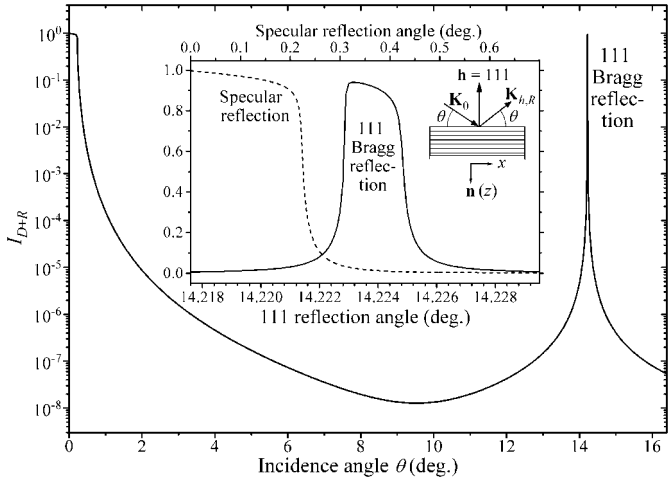

Figure 1
Calculated profiles of the scattering intensity from silicon 111 reflection under unit incidence. Inset: magnified rocking curve around the Bragg angle of 111 reflection (solid line) and the specularly reflected intensity in the grazing-incidence range (dashed line).

is very close to 90° ($\sin 2\theta_B \rightarrow 0$) (Caticha & Caticha-Ellis, 1982). However, the method illustrated above completely solves this problem since the use of θ_B is completely avoided. For simplicity, here we artificially change Si (111) spacing to $d = \lambda/2$ such that $\theta_B = 90°$. While keeping the other parameters unchanged, we have calculated the corresponding rocking curve (using either σ or π polarization), as plotted in Fig. 2. As expected, the full width at half-maximum (FWHM) of the peak is extremely wide while the reflectivity is significantly low. Meanwhile, the peak shift from the Bragg angle completely disappears in the backward diffraction process. Although not shown here, the weak intensity profile corresponding to $\theta_B = 45°$ and π polarization can also be strictly calculated with the current method.

In the above treatment, it is apparent that one diffracted wave inside the crystal is related to the specular reflection from the inner side of the crystal surface. This wave naturally is very weak for non-grazing diffraction. From the configuration of the four internal wavevectors depicted in Fig. 3, one can readily distinguish this wave [labeled with (2)] from the normal one [labeled with (1)] as it has a positive value of $\mathrm{Re}(k_{hz})$ and, accordingly, a larger $\mathrm{Re}(\delta)$ [while the latter has a negative $\mathrm{Re}(k_{hz})$]. For non-grazing geometry, therefore, one can strictly solve the dispersion equation and then use the classical dynamical theory to treat the normal wavefield (ignoring the specularly reflected ones inside and outside the crystals). For instance, the reflectivity in the above examples is, to a high accuracy, equal to $|r_1|^2$ (after sorting) except in the grazing-incidence angular range. Here for universality, we do not use this simplified scheme.

The rigorous method may be conveniently used to treat non-coplanar cases since it is based on vector algebra. A typical instance of non-coplanar diffraction is grazing-incidence diffraction (GID) from lattice planes perpendicular to the crystal surface. The GID geometry is shown in inset I of Fig. 4, where the incidence direction is determined by two angular parameters, θ and Φ_0, *i.e.* $\mathbf{s}_0 = \cos\Phi_0 \cos\theta \mathbf{x} + \cos\Phi_0 \sin\theta \mathbf{y} + \sin\Phi_0 \mathbf{n}$, where $\mathbf{x}$ and $\mathbf{y}$ are unit vectors along x and y axes, respectively. Based on slight approximations, the boundary conditions of the GID geometry for both σ- and π-polarization states are nearly the same as (21) (Holý, 1996). Thus, the above computational procedure can also be used for the GID geometry. Fig. 4 shows the calculated $I_R = |E_R|^2$ and $I_D = |E_D|^2$ for the 220 reflection of a semi-infinite silicon crystal [$\chi_h = \chi_{\bar{h}} = -(9.495 + i0.3504) \times 10^{-6}$]. The two intensity profiles were calculated at $\theta \equiv \theta_B$ for σ polarization. The I_D intensity is actually identical to that calculated by Afanas'ev & Melkonyan (1983). Note that when $|\mathbf{K}_{h\|}| > K$ the second equation of (20) loses its physical meaning since the diffracted wavevector in vacuum should be real. Inset II of Fig. 4 shows the two-dimensional distribution of the diffracted intensity I_D as a function of θ and Φ_0. The blank area labeled 'forbidden region' is the angular range where $|\mathbf{K}_{h\|}| > K$ so that no diffracted wave exists above the crystal surface, which corresponds to transmission geometry.

The representative examples demonstrated above clearly indicate the general validity of the rigorous method. By considering all the four wavefields inside the crystal, one can easily extend it to calculate the diffracted or reflected intensity

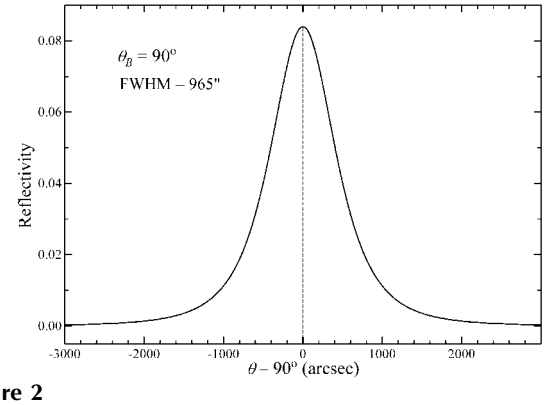

Figure 2
Rocking curve for Bragg angle $\theta_B = 90°$.

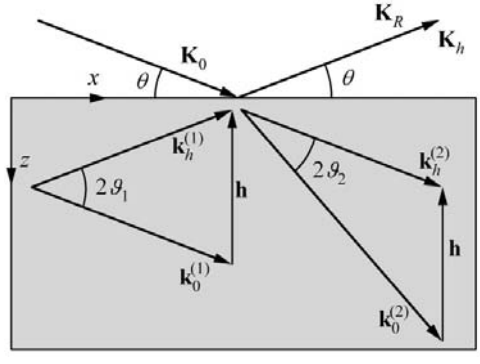

Figure 3
Propagation directions of the waves (represented by their wavevectors) involved in the Bragg case (semi-infinite-crystal case). For symmetric reflection with $\theta \simeq \theta_B$, $\mathbf{K}_0 \parallel \mathbf{k}_0^{(1)} \parallel \mathbf{k}_h^{(2)}$ and $\mathbf{k}_h^{(1)} \parallel \mathbf{K}_h$ (nearly). Note that, for π polarization, $C_\pi^{(1)} = \cos 2\theta_1$ and $C_\pi^{(2)} = \cos 2\theta_2$ may be quite different.

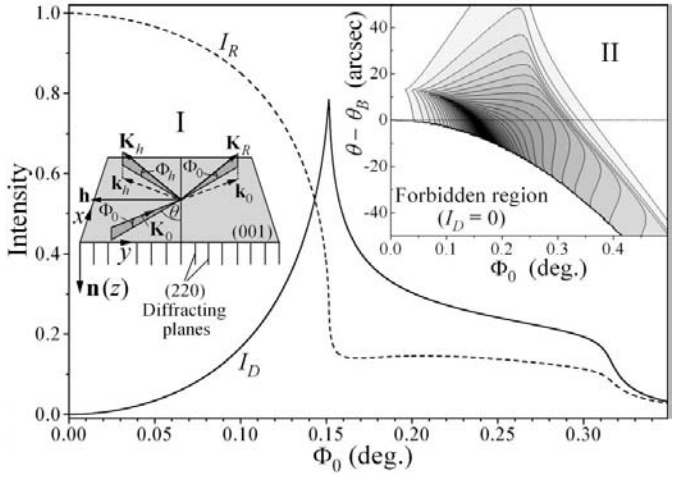

Figure 4
Intensity profiles of the diffracted and specularly reflected beams in the GID geometry of silicon 220 reflection (Φ_0 scan at $\theta = \theta_B$, corresponding to the horizontal dashed line in inset II). Inset I: diffraction setup. Inset II: contour map of I_D as a function of θ and Φ_0. Cu $K\alpha_1$ radiation, σ polarization.

from thin films or multilayers. In these cases, the combination of this method with the recursion matrix method developed by Stepanov *et al.* (1998) is particularly powerful since it can treat both thin and thick crystals/films identically. Although the computation speed of the complete calculation process is reduced (mainly for multilayers), the reduction is not remarkable on a modern personal computer since all the expressions involved have analytical forms.

Note that, in the dynamical theory based purely on the **E** waves, the two denominators in (1) are replaced by K^2 based on the approximation $\nabla(\chi\mathbf{E}) \simeq 0$ (Miyake, 1974; Holý, 1996). In this case, the coefficients of the quartic dispersion equation may be slightly different but the mathematical treatment is the same as that for the **D** waves.

In summary, we have illustrated that the dispersion equation of two-beam X-ray dynamical diffraction is a complex quartic equation that can be strictly solved with a simple and straightforward method. In this method, all the intrinsic diffraction properties are automatically treated. Consequently, a small but universal subroutine may be established and incorporated into any computational procedure to accurately calculate the diffraction quantities for an arbitrary two-beam diffraction geometry.

The authors are grateful to Professor A. Authier for very helpful discussions.

References

Afanas'ev, A. M. & Melkonyan, M. K. (1983). *Acta Cryst.* A**39**, 207–210.

Authier, A. (1998). *Cryst. Res. Technol.* **33**, 517–533.

Authier, A. (2001). *Dynamical Theory of X-ray Diffraction. International Union of Crystallography Monographs on Crystallography*, No. 11. IUCr/Oxford University Press.

Bedynska, T. (1973). *Phys. Status Solidi A*, **19**, 365–372.

Caticha, A. (1993). *Phys. Rev. B*, **47**, 76–83.

Caticha, A. & Caticha-Ellis, S. (1982). *Phys. Rev. B*, **25**, 971–983.

Chien, H. C., Gau, T. S., Chang, S. L. & Stetsko, Y. P. (1999). *Acta Cryst.* A**55**, 677–682.

Colella, R. (1991). *Phys. Rev. B*, **43**, 13827–13832.

De Caro, L., Giannini, G. & Tapfer, L. (1997). *Phys. Rev. B*, **56**, 9744–9752.

De Caro, L. & Tapfer, L. (1997). *Phys. Rev. B*, **55**, 105–112.

Härtwig, J. (1978). *Krist. Tech.* **13**, 1117–1126.

Holý, V. (1996). *X-ray and Neutron Dynamical Diffraction: Theory and Applications*, edited by A. Authier, S. Lagomarsino & B. K. Tanner, pp. 33–42. New York: Plenum.

Laue, M. von (1960). *Röntgenstrahl-Interferenzen*, pp. 334–336. Frankfurt am Main: Akademische Verlagsgesellschaft.

Miyake, S. (1974). *Acta Cryst.* A**30**, 103–104.

Pinsker, Z. G. (1978). *Dynamical Scattering of X-rays in Crystals.* Berlin: Springer-Verlag.

Stepanov, S. A., Kondrashkina, E. A., Köhler, R., Novikov, D. V., Materlik, G. & Durbin, S. M. (1998). *Phys. Rev. B*, **57**, 4829–4841.

Weisstein, E. W. (1999). http://mathworld.wolfram.com/QuarticEquation.html.